1-2018

Arabidopsis *ACTIN-DEPOLYMERIZING FACTOR3* Is Required for Controlling Aphid Feeding from the Phloem

Hossain A. Mondal
University of North Texas

Joe Louis
University of North Texas, joelouis@unl.edu

Lani Archer
University of North Texas

Monika Patel
University of North Texas

Vamsi J. Nalam
Purdue University

See next page for additional authors

Authors
Hossain A. Mondal, Joe Louis, Lani Archer, Monika Patel, Vamsi J. Nalam, Sujon Sarowar, Vishala Sivapalan, Douglas D. Root, and Jyoti Shah

Arabidopsis *ACTIN-DEPOLYMERIZING FACTOR3* Is Required for Controlling Aphid Feeding from the Phloem[1][OPEN]

Hossain A. Mondal,[a,c] Joe Louis,[a,d] Lani Archer,[a,b] Monika Patel,[a,b] Vamsi J. Nalam,[a,e] Sujon Sarowar,[a,2] Vishala Sivapalan,[a] Douglas D. Root,[a] and Jyoti Shah[a,b,3]

[a]Department of Biological Sciences, University of North Texas, Denton, Texas 76203
[b]BioDiscovery Institute, University of North Texas, Denton, Texas 76203
[c]Uttar Banga Krishi Viswavidyalaya, Pundibari, Cooch Behar 736165, India
[d]Department of Entomology and Department of Biochemistry, University of Nebraska, Lincoln, Nebraska 68583
[e]Department of Biology, Indiana University-Purdue University, Fort Wayne, Indiana 46805

ORCID IDs: 0000-0002-6738-6003 (D.D.R.); 0000-0002-5604-1771 (J.S.).

The actin cytoskeleton network has an important role in plant cell growth, division, and stress response. Actin-depolymerizing factors (ADFs) are a group of actin-binding proteins that contribute to reorganization of the actin network. Here, we show that the Arabidopsis (*Arabidopsis thaliana*) *ADF3* is required in the phloem for controlling infestation by *Myzus persicae* Sülzer, commonly known as the green peach aphid (GPA), which is an important phloem sap-consuming pest of more than fifty plant families. In agreement with a role for the actin-depolymerizing function of ADF3 in defense against the GPA, we show that resistance in *adf3* was restored by overexpression of the related ADF4 and the actin cytoskeleton destabilizers, cytochalasin D and latrunculin B. Electrical monitoring of the GPA feeding behavior indicates that the GPA stylets found sieve elements faster when feeding on the *adf3* mutant compared to the wild-type plant. In addition, once they found the sieve elements, the GPA fed for a more prolonged period from sieve elements of *adf3* compared to the wild-type plant. The longer feeding period correlated with an increase in fecundity and population size of the GPA and a parallel reduction in callose deposition in the *adf3* mutant. The *adf3*-conferred susceptibility to GPA was overcome by expression of the *ADF3* coding sequence from the phloem-specific *SUC2* promoter, thus confirming the importance of *ADF3* function in the phloem. We further demonstrate that the *ADF3*-dependent defense mechanism is linked to the transcriptional up-regulation of *PHYTOALEXIN-DEFICIENT4*, which is an important regulator of defenses against the GPA.

In eukaryotes, the actin cytoskeleton, which is composed of filamentous (F)-actin, has a central role in multiple cellular processes, including cell growth, division and differentiation, regulation of polarity, and facilitating cytoplasmic streaming, organelle movement and response to the environment (Staiger, 2000; Hussey et al., 2006; Staiger and Blanchoin, 2006; Pollard and Cooper, 2009; Szymanski and Cosgrove, 2009; Day et al., 2011; Henty-Ridilla et al., 2013). This microfilament network is dynamic and requires continuous reorganization. Remodeling of the actin network involves severing, depolymerization, and polymerization of F-actin, which needs to be spatially and temporally regulated. A variety of actin-binding proteins are involved in remodeling of the actin cytoskeleton (Hussey et al., 2006). These include the actin-nucleating and filament-stabilizing proteins like the formins and fimbrins, respectively, and the actin-depolymerizing factor (ADF) family of proteins (Vidali et al., 2009; Ye et al., 2009; Wu et al., 2010). As a result of their ability to sever and depolymerize F-actin and yield products with ends that can serve as sites for new filament initiation, the ADFs, which are small proteins (approximately 17 kD), increase the dynamics of the actin cytoskeleton and the balance of F-actin versus the free globular (G)-actin (Andrianantoandro and Pollard, 2006; Pavlov et al., 2007). ADFs are also involved in shuttling actin into the nucleus (Nebl et al., 1996; Jiang et al., 1997), where actin is a component of chromatin-remodeling activities that control gene expression (Farrants, 2008; Jockusch et al.,

[1] This work was partially supported by a grant from the National Science Foundation (IOS-0919192) to J.S. M.P. was supported by graduate assistantship from the University of North Texas.
[2] Current address: Botanical Genetics, Buffalo, NY 14203.
[3] Address correspondence to jyoti.shah@unt.edu.
The author responsible for distribution of materials integral to the findings presented in this article in accordance with the Journal policy described in the Instructions for Authors (http://www.plantphysiol.org) is Jyoti Shah (jyoti.shah@unt.edu).
H.A.M., J.L., L.A., M.P., D.D.R., and J.S. conceived and designed the study; H.A.M., J.L., L.A., M.P., V.J.M., S.S., and V.S. conducted the experiments and analyzed and interpreted the data; D.D.R. contributed to methods development and data analysis; the manuscript was written by H.A.M., J.L., and J.S. with input from all authors.
[OPEN] Articles can be viewed without a subscription.
www.plantphysiol.org/cgi/doi/10.1104/pp.17.01438

2006). In addition to the cytosol, some ADFs also localize to the nucleus (Ruzicka et al., 2007).

The *ADF* family in Arabidopsis consists of 11 expressed genes, which based on their relatedness to each other have been grouped into four subclasses (Feng et al., 2006). These *ADF* subclasses exhibit novel and differential tissue-specific and developmental expression patterns (Ruzicka et al., 2007). For example, the subclass I genes, which include *ADF1*, *ADF2*, *ADF3*, and *ADF4*, are constitutively expressed in a variety of vegetative and reproductive tissues, including roots, leaves, flowers, and young seedlings. Among the subclass I genes, *ADF3* was the most strongly expressed. The subclass II genes can be subdivided into clade IIa (*ADF7* and *ADF10*) and clade IIb (*ADF8* and *ADF11*). *ADF7* and *ADF10* exhibit high levels of expression in the reproductive tissues, with strongest expression in mature pollen grain. In comparison, expression of the clade IIa genes is relatively poor in roots and leaves. By contrast, the clade IIb *ADF8* and *ADF11* genes show highest expression in epidermal cells that develop into root hairs. *ADF5* and *ADF9*, which belong to subclass III, exhibit strongest expression in the fast-growing tissues, including the root meristem and emerging leaves. *ADF6*, which is the lone member of subclass IV, is expressed in all tissues including pollen. Biochemical characterization of Arabidopsis ADFs indicated that all class I, II, and IV ADFs possess F-actin-severing/depolymerizing activity, with class I ADFs possessing the strongest activities (Nan et al., 2017). In comparison, the class III ADFs lacked F-actin-severing/depolymerizing activity, and instead possessed F-actin bundling activity (Nan et al., 2017).

ADFs and actin cytoskeleton dynamics are involved in plant response to pathogens. In Arabidopsis, the actin polymerization inhibitor cytochalasin E attenuated nonhost resistance against *Blumeria graminis* f. sp. *tritici* (Yun et al., 2003). Cytochalasin E also interfered with the targeting of the resistance protein RPW8.2 to the extrahaustorial membrane in Arabidopsis inoculated with the powdery mildew *Golovinomyces* spp. fungi (Wang et al., 2009). Similarly, RPW8.2 localization was also affected in plants overexpressing *ADF6*, thus suggesting that the specific targeting of RPW8.2 to the extrahaustorial membrane is dependent on actin cytoskeleton dynamics (Wang et al., 2009). Arabidopsis *ADF4* is required for resisting infection by the bacterial pathogen *Pseudomonas syringae* pv tomato DC3000 expressing the AvrPphB effector protein (Tian et al., 2009). *ADF4* function in defense against this pathogen was linked to the transcriptional regulation of the Arabidopsis *RPS5* gene, which encodes a resistance protein that facilitates the recognition of the AvrPphB effector protein and the activation of downstream defense signaling (Porter et al., 2012). Thus, it was suggested that *ADF4* links actin cytoskeleton dynamics to pathogen perception and defense activation (Porter et al., 2012). *ADF4* was also shown to regulate actin dynamics and callose deposition in response to elf26, a microbial elicitor of immunity (Henty-Ridilla et al., 2014). In contrast, knockdown of *ADF4* resulted in enhanced resistance against an Arabidopsis adapted strain of the powdery mildew fungus (Inada et al., 2016), while knockdown of *ADF2* resulted in enhanced resistance to the root-knot nematode *Meloidogyne incognita* (Clément et al., 2009). Hence, there is a wider involvement of ADFs in plant defense as well as susceptibility to pests.

Aphids (Hemiptera: Aphididae) encompass a large group of insects that consume phloem sap. Nearly 250 species of aphids are considered pests of plants that limit plant growth and productivity due to removal of nutrients from sieve elements and their ability to alter source-sink patterns and thus the flow of nutrients to growing parts of the infested plant (Pollard, 1973; Blackman and Eastop, 2000; Goggin, 2007). Furthermore, some aphids also vector viral diseases (Kennedy et al., 1962; Matthews, 1991; Guerrieri and Digilio, 2008). Aphids utilize their mouthparts, which are modified into slender stylets, to feed from the sieve elements. Prior to inserting stylets into the plant tissue, aphids utilize chemosensory hairs on their antennae to assess the plant surface, potentially for gustatory cues (Powell et al., 2006). Subsequently, the stylets briefly penetrate nonvascular cells to sample cell contents for additional gustatory cues. The puncturing of nonvascular cells along the path of the stylet penetration likely results in the activation of host defenses that could potentially interfere with the ability of the stylet to reach a sieve element. Aphids produce two distinct salivary secretions that facilitate infestation (Miles, 1999). The proteinaceous gelling saliva, which is released by the stylets on their way to the sieve elements, forms a sheath that facilitates stylet movement through the plant tissue and simultaneously minimizes wound responses in the plant by quickly sealing off wounds. In comparison, the watery saliva, which is released when the stylets penetrate the sieve elements, contains factors suggested to enable the insect to prevent and maybe reverse phloem occlusion and thus facilitate feeding from the sieve elements (Miles, 1999; Will et al., 2007, 2009).

The plant surface provides the first line of defense (e.g. trichomes and glandular secretions) that could deter aphid settling on a plant (Walling, 2008). In addition, during the different stages of stylet penetration into the plant tissue, the insect encounters defenses that deter feeding and adversely impact insect fecundity (Walling, 2008; Louis and Shah, 2013). These include factors that contribute to sieve element occlusion (e.g. callose deposition and phloem protein aggregation) as well as insecticidal factors present in the phloem sap (Pedigo, 1999; Smith, 2005; Powell et al., 2006; Goggin, 2007; Walling, 2008). The interaction between Arabidopsis and the green peach aphid (GPA; *Myzus persicae* Sülzer) has been utilized as a model system to characterize plant genes and mechanisms that contribute to defense (Louis et al., 2012; Louis and Shah, 2013). GPA is a polyphagous insect that is an important pest of more than 400 plant species belonging to over 50 plant

families, and the vector of more than 100 viral diseases (Kennedy et al., 1962; Matthews, 1991; Blackman and Eastop, 2000). The *PHYTOALEXIN-DEFICIENT4* (*PAD4*) gene is an important regulator of Arabidopsis defenses that deters GPA feeding and adversely impacts GPA fecundity (Pegadaraju et al., 2005, 2007; Louis et al., 2010a). Genetic studies have indicated that the up-regulation of *PAD4* expression in response to GPA infestation correlated with *PAD4*'s involvement in deterring GPA feeding from sieve elements. This feeding deterrence was intensified in plants overexpressing *PAD4* from the *Cauliflower mosaic virus 35S* gene promoter (Pegadaraju et al., 2007). In contrast, basal expression of *PAD4* was sufficient for the accumulation of an antibiotic activity that adversely impacts insect fecundity (Louis et al., 2010a, 2012).

ADF proteins and profilin, an actin-binding protein that influences actin polymerization, have been identified in phloem exudates from a variety of plants (Schobert et al., 1998, 2000; Kulikova and Puryaseva, 2002; Lin et al., 2009; Rodriguez-Medina et al., 2011; Fröhlich et al., 2012). Furthermore, microfilament meshwork has been revealed in sieve elements of fava bean (*Vicia faba*) injected with the actin-binding fluorescent phalloidin (Hafke et al., 2013). Immunolabeling with anti-actin antibodies further confirmed the presence of actin cytoskeleton in the sieve elements (Hafke et al., 2013). The identification of an actin-binding protein in aphid saliva has led to the suggestion that an actin-dependent process contributes to plant defense in the phloem and aphids' attempt to curtail these defenses by targeting actin dynamics (Nicholson et al., 2012). We therefore investigated the contribution of *ADF* genes in the interaction of Arabidopsis with the GPA. We show that an *ADF3*-dependent mechanism is required for controlling GPA feeding from the sieve elements. We further demonstrate that the *PAD4* gene is a critical downstream component of this *ADF3*-dependent defense mechanism.

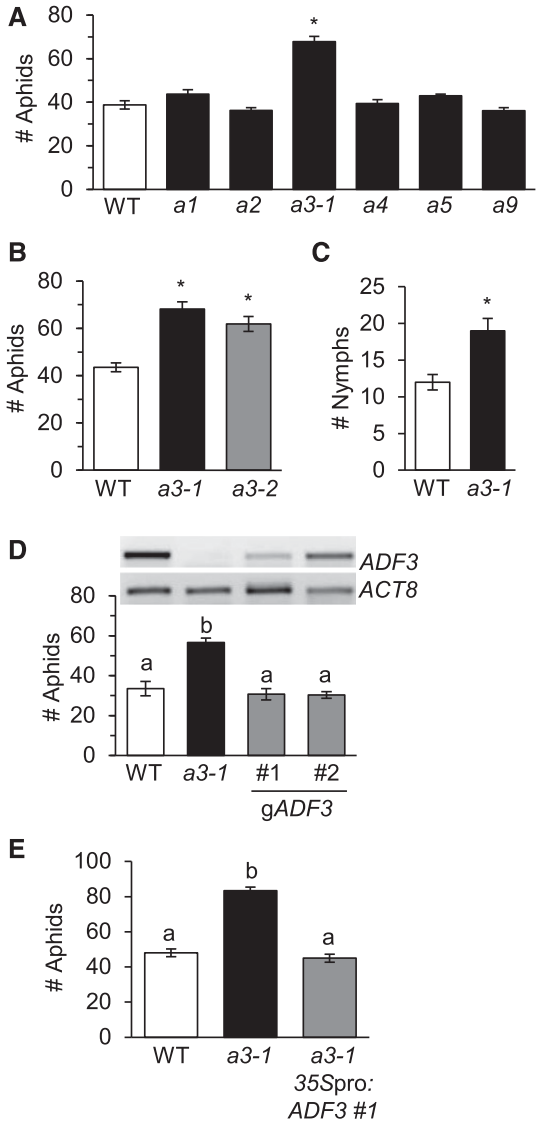

Figure 1. Arabidopsis *ADF3* gene is required for limiting GPA infestation. A, GPA population size on Arabidopsis wild-type (WT) accession Col-0 and *adf1* (*a1*), *adf2* (*a2*), *adf3-1* (*a3-1*), *adf4* (*a4*), *adf5* (*a5*), and *adf9* (*a9*) mutants ($n = 10$) 2 d post-infestation. B, GPA population size on WT accession Col-0 and *adf3-1* (*a3-1*) and *adf3-2* (*a3-2*) mutant plants ($n = 10$) 2 d post-infestation. C, One nymph was released on each WT and *a3-1* plant, and the number of progeny nymphs produced by each insect over a 10-d period was determined ($n = 6$). D, GPA population size on WT accession Col-0, *a3-1* mutant, and two independently derived g*ADF3* plants in which a genomic clone of *ADF3* was transformed into the *a3-1* mutant ($n = 6$). Top panel shows RT-PCR analysis of *ADF3* and as a control *ACT8* expression in uninfested plants of indicated genotypes. E, GPA population size on WT, *adf3-1*, and a transgenic *35S*pro:*ADF3* line #1 in which the *ADF3* coding sequence was expressed from the heterologous *35S* promoter ($n = 6$). See Supplemental Figure S2 for results from an independently derived *35S*pro:*ADF3* line. In A, B, D, and E, twenty adult apterous aphids were released on each plant and the population size (adults + nymphs) on each plant determined 2 d later. All values are mean ± SE for each genotype. In A and B, asterisks above bars denote values that are significantly different from the WT ($P < 0.05$; Dunnett test). In C, an asterisk denotes significant difference from the WT ($P < 0.05$; *t* test). In D and E, different letters above bars denote values that are significantly different from each other ($P < 0.05$; Tukey test).

RESULTS

ADF3 Is Required for Limiting GPA Infestation on Arabidopsis

To determine if the *ADF* genes influence infestation of Arabidopsis by the GPA, Arabidopsis lines that were previously shown to lack or accumulate reduced levels of the *ADF1* (At3g46010), *ADF2* (At3g46000), *ADF3* (At5g59880), *ADF4* (At5g59890), *ADF5* (At2g16700), and *ADF9* (At4g34970) transcripts (Clément et al., 2009; Tian et al., 2009) were utilized in no-choice bioassays with the GPA. For the no-choice bioassay, twenty adult apterous asexually reproducing insects were released on each plant and the insect population size (adults + nymphs) determined 2 d post-infestation. As shown in Figure 1, A and B, only plants lacking *ADF3* function repeatedly showed GPA numbers that were significantly higher than GPA numbers on the wild-type

plant. Compared to the wild-type plant, the GPA population was significantly larger ($P < 0.05$) on the *adf3-1* (Salk_139265) and *adf3-2* (SAIL_501_F01) mutants. *adf3-1* and *adf3-2* contain T-DNA insertions within the first intron and last exon of *ADF3*, respectively (Supplemental Fig. S1A), which is associated with reduced accumulation of the *ADF3* transcript in these mutant lines compared to the wild type (Supplemental Fig. S1B). The increase in GPA population on the *adf3-1* mutant correlated with the significantly higher fecundity of GPA on the mutant compared to the wild type (Fig. 1C). Compared to an average of 1.2 nymphs/day produced by a GPA on the wild-type plant, 1.9 nymphs/day were produced on the *adf3-1* mutant.

To confirm that loss of *ADF3* function is indeed responsible for the better performance of the GPA on the *adf3* plants compared to the wild-type plants, a genomic clone of *ADF3* was transformed into the *adf3-1* mutant. As shown in Figure 1D, *ADF3* expression was restored in two independently derived g*ADF3* transgenic lines. In comparison to the *adf3-1* mutant, the GPA population size was significantly lower on these g*ADF3* transgenic lines and comparable to that on the wild-type plants (Fig. 1D). Similarly, resistance was restored in *adf3-1* plants expressing *ADF3* from the heterologous *Cauliflower mosaic virus 35S* gene promoter. The GPA population size on two independently derived *35S*pro:*ADF3* (in *adf3-1* background) lines was significantly smaller than that on the *adf3-1* mutant and comparable to that on the wild-type plant (Fig. 1E; Supplemental Fig. S2). Taken together, these results confirm that *ADF3* has a critical role in limiting GPA infestation on Arabidopsis.

Actin Cytoskeleton Destabilizers Restore Resistance to the *adf3* Mutant

ADF3 is an actin-binding protein that was recently shown to possess F-actin-severing/depolymerizing activity (Nan et al., 2017). F-actin depolymerization assays conducted by us confirm the ability of ADF3 to depolymerize F-actin (Supplemental Fig. S3). To determine if ADF3-dependent actin reorganization is critical for controlling GPA infestation, the ability of the actin cytoskeleton destabilizers cytochalasin D and latrunculin B to compensate for ADF3 deficiency in the *adf3-1* mutant was evaluated. Two adult aphids were caged onto cytochalasin D- and latrunculin B-treated, and as control on dimethyl sulfoxide (DMSO)-treated leaves of *adf3-1* and wild-type plants, and the number of nymphs born per adult aphid monitored 2 d later. As expected, a significantly larger number of nymphs were born on the DMSO-treated *adf3-1* compared to the wild-type plant (Fig. 2A). However, compared to DMSO treatment, significantly fewer nymphs were born on *adf3-1* leaves that were treated with cytochalasin D and latrunculin B. The number of nymphs born on the cytochalasin D- and latrunculin B-treated *adf3-1* leaves was comparable to that observed on the cytochalasin D- and latrunculin B-treated leaves of wild-type plants, thus indicating that these actin

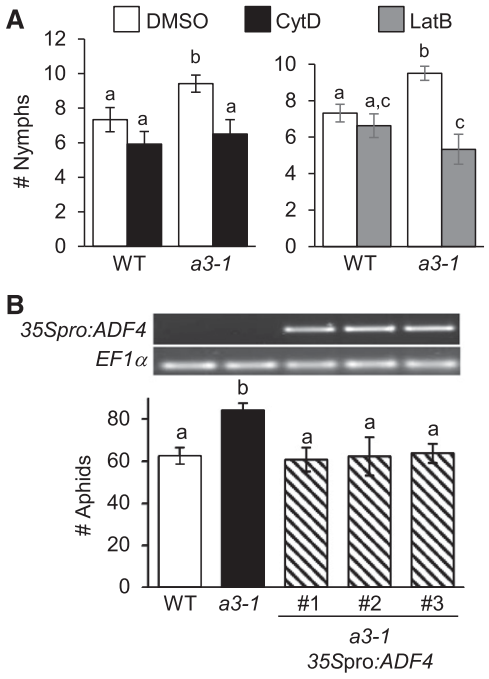

Figure 2. Actin cytoskeleton destabilizers restore resistance to GPA in the *adf3* mutant. A, Effect of the actin destabilizers cytochalasin D (CytD, left) and latrunculin B (LatB, right) on insect numbers. Number of nymphs on leaves of wild type (WT) and *adf3-1* (*a3-1*) mutant treated with 2 μM CytD or LatB and as control with DMSO (0.5%), which was used as a solvent for CytD and LatB. The number of nymphs per adult was determined 2 d after release of two adult aphids on each leaf (n = 12). B, Complementation of *adf3-1*-conferred susceptibility to GPA by constitutive expression of *ADF4* from the *35S* promoter. Top, RT-PCR analysis of *ADF4* expression from the *35S* promoter in three independent *a3-1 35S*Ppro:*ADF4* lines and as control in WT and *a3-1* plants. *EF1α* expression provided the control for RT-PCR. Bottom, no choice assay comparing aphid numbers 2 d post-release of 20 adult aphids per leaf on the WT, *a3-1*, and three independently derived *a3-1 35S*pro:*ADF4* transgenic lines. Values are mean ± SE of a minimum of six replicates for each genotype. Different letters above bars denote values that are significantly different from each other ($P < 0.05$; Tukey test).

destabilizers compensate for the lack of ADF3 function in the *adf3-1* mutant. Taken together, these results confirm the importance of ADF3's actin-depolymerizing function in Arabidopsis defense against the GPA.

To further test the involvement of *ADF3*'s actin-depolymerizing function in controlling GPA infestation, we tested if the *adf3-1* defect could be compensated by overexpression of another actin depolymerizing factor, ADF4 (Henty et al., 2011; Henty-Ridilla et al., 2014; Nan et al., 2017), which exhibits 83% identity and 91% similarity to ADF3 (Supplemental Fig. S4). A previously described *35S*pro:*ADF4* construct (Henty-Ridilla et al., 2014), in which the *ADF4* protein coding sequence is expressed from the *35S* promoter, was transformed into the *adf3-1* mutant. No choice assays were conducted on three independently derived *adf3-1 35S*pro:*ADF4* lines and as a control on the wild type and *adf3-1* mutant. As shown in Figure 2B, GPA

population size was comparable on the wild type and the *adf3-1 35S*pro:*ADF4* plants, and significantly lower than that on the *adf3-1* mutant, thus confirming the ability of *ADF4* overexpression to overcome the *adf3-1* defect in limiting GPA infestation. Collectively, the above results in conjunction with the studies of Nan et al. (2017) lead us to conclude that the impact of *ADF3* on controlling GPA population size is linked to ADF3's function in actin cytoskeleton reorganization.

ADF3 Expression in the Phloem Is Required for Controlling GPA Infestation

ADF3 expression was reported to be the strongest among the *ADF* family of genes in Arabidopsis (Ruzicka et al., 2007). Gene expression data available on the Arabidopsis eFP Browser (http://bbc.botany.utoronto.ca/efp/cgi-bin/efpWeb.cgi) revealed that *ADF3* is expressed throughout the development of Arabidopsis in most organs, except pollen. Furthermore, biotic stress, including GPA infestation did not have a pronounced effect on *ADF3* expression (http://bbc.botany.utoronto.ca/efp/cgi-bin/efpWeb.cgi). Real-time RT-PCR analysis confirmed that *ADF3* expression was not significantly different between uninfested and GPA-infested plants (Fig. 3A). Histochemical analysis for GUS activity in leaves of transgenic *ADF3*pro:*UidA* plants in which the bacterial *UidA*-encoded GUS reporter was expressed from the *ADF3* promoter further confirmed that *ADF3* promoter activity was comparable between uninfested and GPA-infested leaves (Supplemental Fig. S5). *ADF3* promoter activity was strong in the lateral and minor veins compared to the nonvascular tissues (Fig. 3B; Supplemental Fig. S5). Within the vasculature, GUS activity was found to be strong in the phloem (Fig. 3C).

To test if *ADF3* expression in phloem is important for ADF3's role in controlling GPA infestation, we tested if the *ADF3* coding sequence expressed from the phloem-specific *SUC2* promoter (Gottwald et al., 2000) was sufficient to restore resistance against the GPA in the *adf3-1* mutant background. Transgenic *adf3-1* plants expressing the *ADF3* coding sequence from the *35S* promoter provided the positive controls for this experiment. As shown in Figure 3D, the *SUC2*pro:*ADF3* chimera complemented the *adf3-1* defect. GPA population size was significantly lower on three independently derived *adf3-1 SUC2*pro:*ADF3* lines compared to the *adf3-1* mutant. The level of resistance observed in the *adf3-1 SUC2*pro:*ADF3* lines was comparable to that observed in *adf3-1 35S*pro:*ADF3* line. There, results confirm an important role for *ADF3* in the phloem in controlling GPA infestation on Arabidopsis.

ADF3 Is Required for Limiting GPA Feeding from Sieve Elements

The adverse effect of *ADF3* on insect fecundity could result from its effect on the accumulation of antibiosis

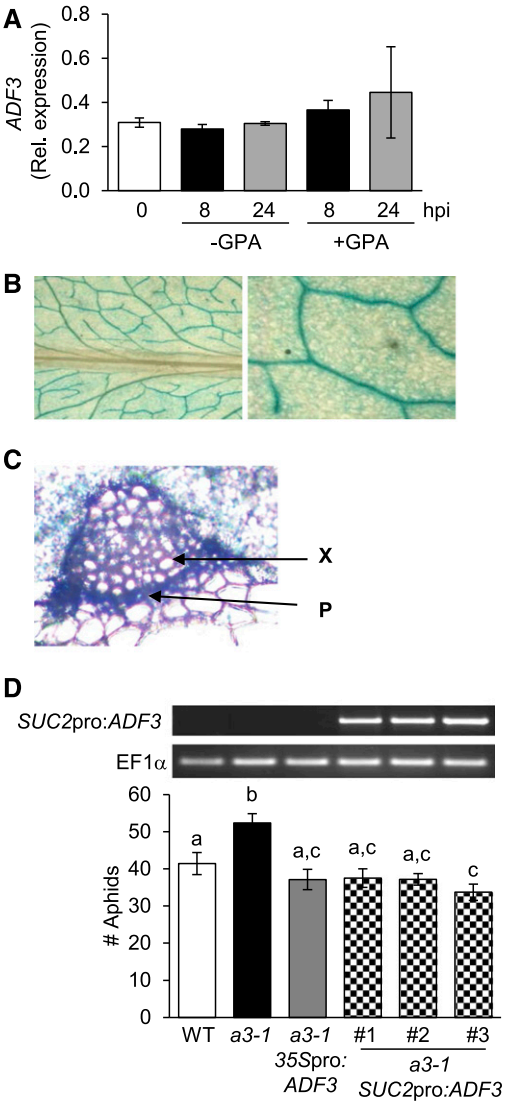

Figure 3. *ADF3* function in the phloem is required for controlling GPA infestation. A, Real-time RT-PCR analysis of *ADF3* expression relative to that of *EF1α* in uninfested (−GPA) and GPA-infested (+GPA) leaves of the Arabidopsis accession Col-0 at the indicated h post-infestation (hpi). Values are mean ± SE ($n = 3$). B, Histochemical staining for GUS activity (blue color) in a GPA-infested leaf of a *ADF3*pro:*UidA* plant in which *UidA* expression is driven from the *ADF3* promoter. Right, close-up showing strong GUS activity in the veins. C, Histochemical staining in a section through a vein showing strong GUS activity in the phloem (P). X, xylem. D, *ADF3* expression in the phloem is sufficient for controlling GPA infestation. Top, RT-PCR analysis of *ADF3* expression from the *SUC2* promoter in three independent *a3-1 SUC2*Pro:*ADF3* lines and as control in wild-type (WT) accession Col-0, *a3-1*, and *a3-1 35S*pro:*ADF3* plants. Primers specific for the *SUC2* promoter-driven *ADF3* construct were used. *EF1α* expression provided the control for RT-PCR. Bottom, GPA population size on Arabidopsis plants of indicated genotypes. Twenty adult apterous aphids were released on each plant and the population size (adults + nymphs) on each plant determined 2 d later. Values are mean ± SE of a minimum of six replicates for each genotype. Different letters above bars denote values that are significantly different from each other ($P < 0.05$; Tukey test).

activity or alternatively due to its impact on the insects feeding behavior. Previous studies have indicated the presence of an antibiotic activity, which is detrimental to GPA fecundity, in leaf petiole exudates that are enriched in phloem sap (Louis et al., 2010a; Nalam et al., 2012). To determine if *ADF3* controls the accumulation of this antibiotic activity, petiole exudates collected from leaves of wild type, and the *adf3-1* and *adf3-2* mutants were added to a synthetic diet and GPAs were reared on the supplemented diet for 5 d. As shown in Figure 4, in comparison to the GPA population on the synthetic diet lacking petiole exudates, insect population size was significantly smaller ($P < 0.05$) on diet supplemented with petiole exudates from wild-type plants. The GPA population size was similarly lower on diet supplemented with petiole exudates collected from the *adf3-1* and *adf3-2* mutant plants, thus confirming that *ADF3* does not significantly influence the accumulation of this antibiotic activity in the phloem sap-enriched petiole exudates.

To test if *ADF3* adversely influences GPA feeding, GPA feeding behavior was monitored on leaves of the wild-type and *adf3-1* mutant plants with the electrical penetration graph (EPG) technique in which the plant and the insect, with a wire glued to its dorsum, are part of a low-voltage circuit (van Helden and Tjallingii, 2000). The different waveform patterns in an EPG are characteristic of the different feeding behavioral activities of the insect. EPG provides information on the time the insect takes to first probe (FP) the plant with its stylets, the time spent by the insect to find and tap into a sieve element for the first time (f-SEP; first sieve element phase), and the sum of time spent during the recording period by the insect in all the SEPs (s-SEP), in the xylem phase (XP) when the stylet is in the xylem and the insect is consuming xylem sap, the pathway phase (PP) when the stylet is inserted into the leaf tissue but is outside the sieve elements and likely sampling other cells, and the nonprobing (NP) phase when the stylet is not inserted into the plant tissue. As shown in Figure 5A,

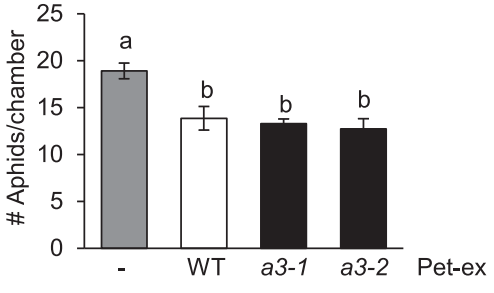

Figure 4. *ADF3* is not required for accumulation of antibiosis activity in petiole exudates. Artificial diet assay showing a comparison of GPA numbers on diet containing petiole exudates (Pet-ex) collected from leaves of wild-type (WT), *adf3-1* (*a3-1*), and *adf3-2* (*a3-2*) plants. Control was an artificial diet supplemented with the buffer used to collect petiole exudates. Values are mean ± SE of a minimum of seven replicates for each treatment. Different letters above bars denote values that are significantly different from each other ($P < 0.05$; Tukey test).

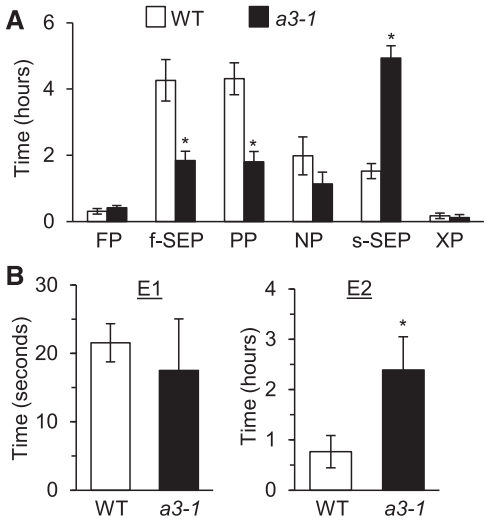

Figure 5. *ADF3* is required for controlling GPA feeding on Arabidopsis leaves. A, Electrical penetration graph (EPG) comparison of time spent by GPA in various activities on the wild-type (WT) and *adf3-1* (*a3-1*) mutant plants in an 8-h period. FP, time taken for first probe; f-SEP, time taken to reach first sieve element phase; PP, time spent in pathway phase during the 8-h period; NP, total time spent nonprobing during the 8-h period; s-SEP, total time spent in sieve element phase during the 8-h period; XP, total time spent in the xylem phase during the 8-h period. B, EPG comparison of time spent by GPA in the E1 (salivation) and E2 (ingestion) phases during the first SEP. In A and B, values are the mean ± SE ($n = 10$). Asterisks indicate significant differences ($P < 0.05$; Kruskal-Wallis test) in an individual feeding parameter between insect feeding on the *a3-1* compared to the WT plant.

comparison of these behavioral activities of the GPA on the wild type and the *adf3-1* mutant revealed that the insect spent significantly less time ($P < 0.05$) attaining the f-SEP on the *adf3-1* mutant. In addition, the s-SEP was significantly longer ($P < 0.05$) when the insects were on the *adf3-1* mutant compared to the wild type, thus indicating that the insects spent significantly more time feeding from the sieve elements of the *adf3-1* mutant than the wild-type plant. A corresponding reduction in the time spent by GPA in PP was observed on the *adf3-1* mutant compared to the wild-type plant, thus confirming that the insect encounters fewer obstacles that allow it to find sieve elements faster and feed for longer periods on the *adf3-1* mutant. In contrast to f-SEP, s-SEP, and PP, the insect took comparable amount of time to reach the FP and spent comparable time in the NP and XP on the wild type and *adf3-1* mutant. These results suggest that *ADF3* and/or an *ADF3*-dependent mechanism(s) interferes with the ability of the GPA to find and feed from the sieve elements.

During the SEP, the watery saliva injected by the insect into the sieve elements may inhibit phloem-sealing mechanisms (Powell et al., 2006; Tjallingii, 2006; Will and van Bel, 2006). This watery saliva injection phase, the E1 phase, is followed by the E2 phloem sap-ingestion phase. A prolonged E1 and/or reduced

E2 is suggestive of a lowered ability of the insect to suppress rapid phloem-sealing mechanisms (Garzo et al., 2002). To determine if insects feeding from sieve elements of the *adf3* mutant encounter less resistance that results in a shorter duration of watery saliva release into the sieve elements, the length of the E1 waveform in the first SEP was compared between insects released on the wild type and the *adf3-1* mutant. As shown in Figure 5B, the length of the E1 phase was comparable between insects placed on the wild type and *adf3-1* mutant, thus indicating that *ADF3* does not influence the length of the period of watery saliva release by GPA into Arabidopsis sieve elements. However, the E2 phase was significantly shorter ($P < 0.05$) on the wild type compared to the *adf3-1*, thus confirming that *ADF3* and/or an *ADF3*-dependent mechanism in the wild-type plant limits ingestion of phloem sap by the GPA.

ADF3 Controls Callose Deposition in GPA-Infested Plants

Callose deposition is one of the processes involved in phloem occlusion (Will and van Bel, 2006; Kempema et al., 2007; Hao et al., 2008). Similarly, callose deposited outside cells that are in the path of the stylets trying to reach the sieve element, could interfere with the ability of the stylets to reach sieve elements. Considering that *ADF3* is required for limiting GPA feeding, and callose synthesis is subject to the participation of the actin cytoskeleton (Cai et al., 2011), we tested the impact of *ADF3* on callose deposition in GPA-infested plants. As shown in Figure 6, in response to GPA infestation, a significant increase in the number of callose spots was observed in wild-type plants. In comparison to the wild type, the number of callose deposits were lower in the GPA-infested leaves of *adf3-1* mutant. The number of callose spots in the GPA-infested *adf3-1* mutant was comparable to that observed in the GPA-infested *pad4-1* mutant (Fig. 6), which, like *adf3-1*, is also defective in controlling GPA feeding from the sieve elements (Pegadaraju et al., 2007; Louis et al., 2012), thus further relating callose deposition with the ability of the plant to control GPA feeding.

An *ADF3*-Dependent Mechanism Controls *PAD4* Expression in GPA-Infested Plants

In the nucleus, actin is a component of the chromatin remodeling complexes that function to regulate gene expression (Jockusch et al., 2006; Farrants, 2008). Furthermore, some ADFs are involved in shuttling actin into the nucleus and thus in regulating gene expression (Nebl et al., 1996; Jiang et al., 1997). We noted that the up-regulation of *PAD4* expression, which is observed in the GPA-infested leaves of the wild type, was attenuated in the *adf3-1* mutant. As shown in Figure 7A, in comparison to the significant ($P < 0.05$) increase in *PAD4* expression observed in GPA-infested compared to uninfested wild-type plants, in the *adf3-1* mutant,

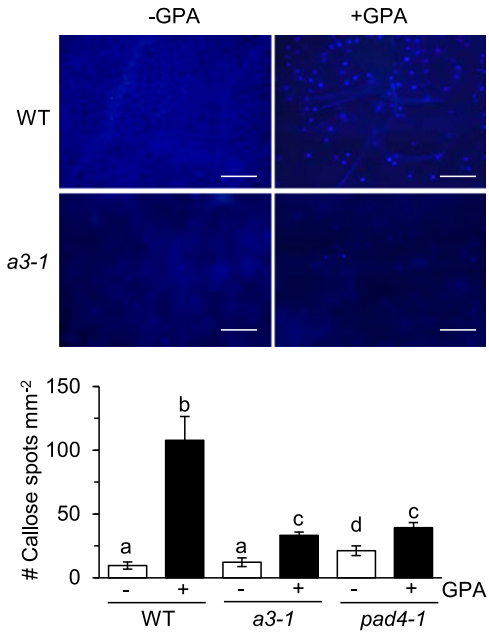

Figure 6. *ADF3* is required for promoting callose deposition in response to GPA infestation. Top, callose deposits (light blue spots) in leaves of wild-type (WT) plants of the Arabidopsis accession Col-0 and the *adf3-1* (*a3-1*) mutant, 24 hpi with the GPA (+GPA) or as control in uninfested (−GPA) plants. Bar = 200 μM. Bottom, mean number of callose spots ± SE per mm^2 of leaf tissue in GPA-infested and uninfested leaves ($n = 5$). Different letters above bars denote values that are significantly different from each other ($P < 0.05$; Tukey test).

PAD4 transcript levels did not exhibit a significant increase in response to GPA infestation. These results suggest that an *ADF3*-dependent mechanism regulates *PAD4* transcript accumulation in GPA-infested wild-type plants.

To further define the relationship between *ADF3* and *PAD4* in Arabidopsis defense against the GPA, *adf3-1 35S*pro*:PAD4* and *pad4-1 35S*pro*:ADF3* plants in which *PAD4* and *ADF3*, respectively, are expressed from the *35S* promoter were generated. *adf3-1 35S*pro*:ADF3* plants provided the controls. As expected, *ADF3* expression from the *35S* promoter restored basal resistance against GPA in the *adf3-1 35S*pro*:ADF3* plants (Fig. 7B; Supplemental Fig. S6). By comparison, in two independently derived transgenic lines, *ADF3* expression from the *35S* promoter was unable to restore resistance in the absence of a functional *PAD4* gene in the *pad4-1 35S*pro *ADF3* plants (Fig. 7B; Supplemental Fig. S6), thus suggesting a critical role for *PAD4* in *ADF3*-dependent defense against the GPA. Moreover, in no-choice assays conducted on plants of two independent *adf3-1 35S*pro *PAD4* lines, GPA population size was comparable to that on the wild-type plants but smaller than on the *adf3-1* mutant (Fig. 7B; Supplemental Fig. S6), thus indicating that overexpression of *PAD4* from the heterologous *35S* promoter is sufficient to restore significant levels of resistance in the absence of *ADF3* function. Collectively, these

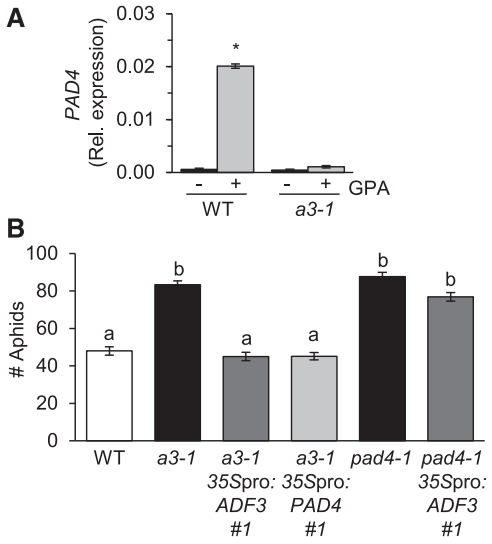

Figure 7. *ADF3* is required for promoting *PAD4* expression in response to GPA infestation. A, qRT-PCR analysis of *PAD4* expression relative to *EF1a* expression at 24 hpi in GPA-infested and uninfested wild-type (WT) and *adf3-1* (*a3-1*) mutant plants. Values are mean ± SE ($n = 3$). Asterisks indicate values that are significantly different from the corresponding mock-treatment ($P < 0.05$; *t* test). B, GPA population size on WT, *a3-1*, *a3-1 35S*pro*:ADF3* line #1, *a3-1 35S*pro*:PAD4* line #1, *pad4-1*, and *pad4-1 3S*pro*:ADF3* line #1. See Supplemental Figure S6 for data for additional independently derived transgenic lines. The no-choice assay was conducted by releasing twenty adult apterous aphids on each plant and the population size (adults + nymphs) on each plant determined 2 d later. Values are mean ± SE ($n = 6$) for each genotype. Different letters above bars denote values that are significantly different from each other ($P < 0.05$; Tukey test).

results reaffirm the importance of *ADF3*-dependent regulation of *PAD4* expression in Arabidopsis defense against the GPA.

DISCUSSION

The actin cytoskeleton and actin-binding proteins are present in the phloem (Schobert et al., 1998, 2000; Kulikova and Puryaseva, 2002; Lin et al., 2009; Rodriguez-Medina et al., 2011; Fröhlich et al., 2012; Hafke et al., 2013). However, their biological function in the phloem is poorly understood. We provide multiple lines of evidence indicating an important role for ADF3 and actin reorganization in Arabidopsis defense against the GPA, particularly in controlling GPA feeding from the sieve elements: (1) Compared to the wild-type plant, GPA population was larger on *adf3* mutant plants. (2) The *adf3* deficiency in controlling GPA infestation was compensated by the actin cytoskeleton destabilizers cytochalasin D and latrunculin B and by overexpression of actin depolymerizing factor ADF4. (3) *ADF3* was expressed in the phloem, and expression of *ADF3* from the phloem-specific *SUC2* promoter was sufficient to restore resistance against the GPA in the *adf3-1* mutant. (4) In agreement with it functioning in the phloem, *ADF3* was required for limiting GPA feeding from the sieve elements. Our results further demonstrate that *ADF3*'s involvement in controlling GPA infestation is in part mediated via its influence on *PAD4* expression and hence defense signaling.

EPG analysis indicated that besides limiting GPA feeding from sieve elements, an *ADF3*-dependent mechanism interferes with the ability of the insect stylets to reach the sieve elements. Thus, we propose that an *ADF3*-dependent process also impacts events occurring prior to the first penetration of a sieve element by the aphid stylets. On their way to finding a sieve element, the stylets penetrate and sample contents of nonvascular cells (Pollard, 1973; Powell et al., 2006). These punctures of plant cells by the stylets could stimulate plant defenses. Salivary components that are released into the plant tissue are also known to stimulate host defenses (DeVos and Jander, 2009; Bos et al., 2010). For example, callose deposition increases in response to GPA infestation (Elzinga et al., 2014) as well as application of GPA-derived elicitors (Prince et al., 2014). Callose has been implicated in the control of infestation by insects that feed from the phloem (Will and van Bel, 2006; Kempema et al., 2007; Hao et al., 2008). Callose deposited in the sieve elements interferes with the ability to the aphid to feed from the sieve elements. In addition, callose deposited outside the sieve elements could interfere with the ability of the stylet to reach sieve elements to further limit insect feeding. The GPA infestation-associated increase in callose deposition was attenuated the *adf3-1* mutant, suggesting an important role for *ADF3* in this process. The actin cytoskeleton is involved in the localization of callose synthases to the cell membrane, presumably due to the involvement of the actin cytoskeleton in vesicular trafficking (Cai et al., 2011). Whether ADF3 is similarly involved in the localization of callose synthase is not known. However, since the GPA infestation-associated increase in callose deposition was also attenuated in the *pad4* mutant, we suggest that the impact of *ADF3* on callose deposition in response to GPA infestation is likely exerted via *ADF3*'s engagement of the *PAD4* defense-signaling pathway. The contribution of *PAD4* in promoting callose deposition is further supported by a recent study, which showed that the endophytic *Bacillus velezensis*-induced resistance against the GPA was accompanied by an increase in callose deposition, which was dependent on *PAD4* (Rashid et al., 2017).

Actin is a component of chromatin remodeling activities that control gene expression in the nucleus (Jockusch et al., 2006; Farrants, 2008), and ADF's are involved in shuttling actin into the nucleus (Nebl et al., 1996; Jiang et al., 1997) and in regulating gene expression (Burgos-Rivera et al., 2008; Porter et al., 2012). Among the subclass I *ADF*s in Arabidopsis, *ADF4*'s involvement in effector-triggered immunity is linked to downstream activation of gene expression (Porter et al., 2012). Similarly, our results indicate that *ADF3*'s involvement in defense against the GPA is linked to the up-regulation of *PAD4*. However, although *PAD4* is required for *ADF3*-conferrred resistance to the GPA, our results also indicate that *ADF3* and *PAD4* have

additional functions in Arabidopsis defense against the GPA that are independent of each other. For example, unlike *PAD4*, an *ADF3*-dependent mechanism hinders with the ability of the insect to find sieve elements. In contrast, unlike *ADF3*, a *PAD4*-dependent mechanism is required for the accumulation of an antibiosis activity in the vascular sap (Pegadaraju et al., 2005, 2007; Louis et al., 2010a). Previous studies have shown that while basal expression of *PAD4* contributes to the antibiosis activity, the up-regulation of *PAD4* expression is associated with the feeding deterrence function of the *PAD4*-dependent pathway (Pegadaraju et al., 2007; Louis et al., 2010a, 2010b). These conclusions are in agreement with the observations described here that *ADF3*, which is required for the up-regulation of *PAD4* expression in response to GPA infestation, but not for the basal expression of *PAD4*, is required for controlling GPA feeding, but not for the accumulation of the antibiotic activity. It is likely that different cell types are involved in exerting these effects. For example, the contribution of *ADF3* and *PAD4* to feeding deterrence is exerted at the level of the sieve elements, while *ADF3*'s involvement in hindering with the ability of the GPA to find sieve elements is exerted outside the sieve elements. Similarly, *PAD4*'s contribution to antibiosis is likely exerted in tissues where these antibiotic factors are produced.

ADF3 (At5g59880) and *ADF4* (At5g59890), which are located in tandem on chromosome 5, are both subclass I ADFs that share a high level of sequence identity. Both possess actin-severing/depolymerizing activity (Henty-Ridilla et al., 2014; Nan et al., 2017). However, while *ADF3*, not *ADF4*, is essential for defense against the GPA, *ADF4*, but not *ADF3*, is required for AvrPphB -triggered immunity against the bacterial pathogen *P. syringae* (Tian et al., 2009). The ability of *ADF4* expressed from the strong and ubiquitously expressed *35S* promoter to limit GPA population in the *adf3-1* mutant background indicates that ADF3 and ADF4 have overlapping biochemical functions. We therefore conclude that the unique biological functions of *ADF3* in defense against the GPA is likely determined by differences in the spatial expression pattern and/or overall level of expression of *ADF3*, compared to *ADF4*, and likely other subclass I *ADF* genes.

CONCLUSION

Our results demonstrate that an *ADF3*-dependent mechanism hinders with the ability of the GPA to find and feed from sieve elements. Considering that *ADF3* is required for up-regulating *PAD4* expression and callose deposition in GPA-infested leaves, we postulate that an *ADF3*-dependent mechanism is involved in signaling associated with Arabidopsis defense against the GPA.

MATERIALS AND METHODS

Plant and Insect Materials

All plants were cultivated at 22°C under a 14-hr light (100 μE m^2 s^{-1}) and 10-hr dark regime on a peat-based soil mix (Fafard #2, fafard.com). The Arabidopsis (*Arabidopsis thaliana*) *adf1* (Salk_144459; Tian et al., 2009), *adf2* (RNAi line; Clément et al., 2009), *adf3-1* (Salk_139265C; Tian et al., 2009), *adf3-2* (SAIL_501_F01), *adf4* (Garlic_823_A11.b.1b.Lb3Fa; Tian et al., 2009), *adf5* (Salk_030145C), and *adf9* (Salk_056064; Tian et al., 2009) lines were used in this study. Silencing of *ADF2* in the *ADF2* RNAi line was induced by treating plants with 0.5% ethanol solution (Clément et al., 2009).

A GPA (Kansas State University, Museum of Entomological and Prairie Arthropod Research, voucher specimen 194) colony was reared at 22°C under a 14-hr light (100 μE m^2 s^{-1}) and10-hr dark regime on a 1:1 mixture of commercially available radish (*Raphanus sativus*; Early Scarlet Globe) and mustard (*Brassica juncea*; FL Broadleaf).

No-Choice Tests

No-choice assays were conducted as previously described (Pegadaraju et al., 2005; Louis et al., 2010a). Unless stated otherwise, 20 adult asexually reproducing apterous (wingless) aphids were placed on each 4-week-old plant. Two days later, the number of insects on each plant was counted. To monitor aphid fecundity, one young nymph (3–4 d old) was placed on each plant, and the total number of progeny born over a 10-d period was recorded.

Monitoring Aphid Feeding Behavior

The EPG technique (van Helden and Tjallingii, 2000; Walker, 2000) was used to simultaneously monitor the feeding behavior of GPA on 4-week-old plants of two different genotypes, as previously described (Pegadaraju et al., 2007). An eight-channel GIGA-8 direct current amplifier (http://www.epgsystems.eu/systems.htm) was used for simultaneous recordings of eight individual aphids. The waveform recordings were analyzed using the EPG analysis software PROBE 3.4 (provided by W.F. Tjallingii, Wageningen University, the Netherlands). The analysis of the first sieve element phase was divided into the length of the first salivation E1 and the time of active ingestion phase E2.

Petiole Exudate Collection and Artificial Diet Feeding Assays

Phloem sap-enriched petiole exudates were collected from Arabidopsis leaves as previously described (Chaturvedi et al., 2008). After concentration, equal volumes of petiole exudates were added to a synthetic diet (Mittler and Dadd, 1965) contained in a feeding chamber (Louis et al., 2010b). Three adult aphids were released on each feeding chamber, and the total number of GPA in each feeding chamber was determined 5 d later.

Actin Cytoskeleton Destabilizer Treatment

Two leaves of each 4-week-old plant were infiltrated with 2 μM of cytochalasin D or latruculin B solubilized in 0.5% dimethyl sulfoxide (DMSO), followed by release of two adult GPA on each leaf. Each leaf was caged in a perforated 2-mL microfuge tube to prevent escape of insects. Total number of nymphs on each leaf were determined 2 d later. Plants treated with 0.5% DMSO provided the negative control. A minimum of twelve leaves of each genotype were used for each treatment.

PCR Analysis for Mutant Screening

All primers used in this study to confirm the knockdown of individual *ADF* genes in the *adf* mutants and the *ADF2* RNAi knockdown lines are listed in Supplemental Table S1. PCR with gene-specific primers was performed under the following conditions: 94°C for 5 min, followed by 36 cycles of 94°C for 30 s, 56°C for 30 s, and 72°C for 1 min, with a final extension of 72°C for 5 min. PCR for genotyping the *adf* mutants utilized the T-DNA left border primer and a gene-specific primer. The PCR conditions included a 5 min denaturation at 94°C, followed by 36 cycles of 94°C for 30 s, 56°C for 30 s, and 72°C for 1 min, with a final extension of 72°C for 5 min.

Gene Expression

RNA extraction from leaves was performed as previously described (Pegadaraju et al., 2005). Each sample included a minimum of two leaves. A minimum of three samples was analyzed for each treatment. For real-time

RT-PCR, gene expression levels were normalized to that of *EF1α*, while for RT-PCR *ACT8* was used as a control. Gene-specific primers used for real-time RT-PCR and RT-PCR are listed in Supplemental Table S1.

Expression and Purification of Recombinant ADF3 Proteins

The primers 5′-CGCCCCATATGGCTAATGCAGCATCAGGAATGGCAG-TCC-3′ and 5′-AAGCTTCTCGAGTCAATTGGCTCGGCTTTTGAAAAC-3′ were used to amplify the *ADF3* coding sequence, using cDNA prepared from mRNA harvested from Arabidopsis Col-0 as the template. The resultant product was digested with *Nde*I and *Xho*I, which cut within the two primer regions. The digested product was ligated between the *Nde*I and *Xho*I sites of pET28a vector. The resultant pET28a-ADF3 plasmid in which a 6X-His tag was incorporated at the N-terminal end of ADF3 was transformed into *Escherichia coli* strain BL21-DE3. Expression of the recombinant ADF3 protein was induced by the addition of Isopropyl-β-D-thio-galactopyranoside (IPTG) prior to bacterial cell harvest. The recombinant, 6X-His-tagged protein was purified over an affinity Ni-NTA column (QIAexpress, Qiagen, http://www.qiagen.com). The purified ADF3 protein was centrifuged at 20,000*g* for 30 min at 4°C before use in the F-actin cosedimentation assays. The GST-ADF3 and GST-ADF4 clones used in the actin depolymerization assays encode recombinant proteins that contain GST fused to the N-terminal end of ADF3 and ADF4. These were a gift of Brad Day. The recombinant proteins were purified over a GST-affinity column before use in actin depolymerization assays.

Transgenic *ADF3*- and *ADF4*-Expressing Plants

The *ADF3* genomic fragment (g*ADF3*) was amplified using the primers 5′-TAAATGAATTTTTTTTACGGGA-3′ and 5′-TCAATTGGCTCGGCTTTTGA-3′, and the resultant product cloned into the pCR8/GW/TOPO vector (Life Technologies; www.lifetechnologies.com). Gateway LR clonase (Life Technologies; www.lifetechnologies.com) was used to mobilize the cloned fragment into the binary vector pMDC107 (Curtis and Grossniklaus, 2003) to yield pMDC107-gADF3. To generate a construct for in planta expression of the *ADF3* coding sequence from the *Cauliflower mosaic virus 35S* gene promoter, the pET28a-ADF3 plasmid (see above) was used as a template with the primer 5′-ATGGGCAGCAGCCATCATC-3′, which is derived from the pET28a vector and primer 5′-TCAATTGGCTCGGCTTTTGA-3′ to amplify the *ADF3* coding region. The resultant PCR product was cloned into pCR8/GW/TOPO, from where it was mobilized into the destination vector pMDC32 (Curtis and Grossniklaus, 2003) to yield the pMDC32-*35S*pro:ADF3 plasmid.

The pMDC107-gADF3 and pMDC32-*35S*pro:ADF3 plasmids were individually electroporated into *Agrobacterium tumefaciens* strain GV3101, which was subsequently used for transforming the *adf3-1* plants by the floral-dip method (Zhang et al., 2006) to generate transgenic plants in which the *adf3-1* mutant phenotype was complemented by expression of the g*ADF3* and *35S*pro:*ADF3*. Transgenic plants were selected on 1/2 strength Murashige and Skoog agar plates containing hygromycin (25 μg mL^{-1}). The *35S*pro:*PAD4* construct has been previously described (Xing and Chen, 2006).

The *35S*pro:*ADF4* construct (Henty-Ridilla et al., 2014), in which the *ADF4* coding sequence containing an N-terminal T7 epitope tag is expressed from the *35S* promoter was used for generating the *adf3-1 35S*pro:*ADF4* plants by transforming *adf3-1* plants with the recombinant construct. Transformed plants were screened based on their resistance to kanamycin (50 μg mL^{-1}), and the presence of the recombinant construct and its expression confirmed by PCR and RT-PCR, respectively. To verify the construct in the *adf3-1* 35S:ADF4 transgenic lines, a forward primer 5′-GGTGGTCAACAAATGGGT- 3′, which is specific to the region containing the T7 tag, and a reverse primer 5′-TTAGTTGACGCGGCTTTTC- 3′, which is specific to the *ADF4* coding sequence, were utilized. The same primers were also utilized to monitor expression of the recombinant constructed by RT-PCR. The PCR conditions were as follows: 94°C for 5 min, followed by 30 cycles of 94°C for 30 s, 56°C for 30 s, and 72°C for 30 s, followed by a final extension step of 72°C for 5 min.

To generate a *SUC2*pro:*ADF3* construct, the *ADF3* coding sequence with a 6X-His tag at the N terminus was amplified from plants containing the g*ADF3* construct, which contains a His tag on the 5′ end. The primers 5′-ATGGG-CAGCAGCCATCATC-3′ and 5′-TCAATTG GCTCGGCTTTTGA-3′ were used to amplify the *ADF3* coding sequence, and the resultant PCR product was cloned into pCR8/GW/TOPO. The pCR8 product was then mobilized into a pMDC85 destination vector (Curtis and Grossniklaus, 2003), which had been modified by the removal of the 2× *35S* promoter and replaced by the SUC2 promoter (Elzinga et al., 2014). The resultant construct, pMDC85-*SUC2*pro:*ADF3*, was transformed into *adf3-1* using *A. tumefaciens* via the floral-dip method (Zhang et al., 2006). Transformed plants were screened based on resistance to hygromycin (20 μg mL^{-1}) and presence of the recombinant construct and its expression confirmed by PCR and RT-PCR, respectively. A forward primer 5′-AGCCATCATCATCATCATCAC-3′ designed to the 6X-HIS tag at the 5′ end of the *ADF3* coding sequence and a reverse primer 5′-TCAATTG GCTCGGCTTTTG-3′ that is specific to the *ADF3* coding sequence were utilized in PCR reactions to confirm the presence of the *SUC2*pro:*ADF3* construct. These same primers were also utilized to monitor expression of the recombinant construct by RT-PCR. The PCR conditions were as follows: 94°C for 5 min, followed by 30 cycles of 94°C for 30 s, 57°C for 30 s, and 72°C for 45 s, followed by a final extension step of 72°C for 5 min.

GUS Reporter Constructs and Histochemical Analysis

A 2,035-bp DNA fragment upstream of the transcriptional start site of ADF3 was amplified with Platinum Taq polymerase (Invitrogen) using Arabidopsis Col-0 genomic DNA as template and the primers 5′-TAAATGAATTTTTTT-TACGGGA-3′ and 5′-GGTTGAATCAAAGCTAGTCTCA-3′. The PCR product was cloned into pCR8/GW/TOPO, from where it was mobilized into the pMDC132 vector (Curtis and Grossniklaus, 2003), which contains the coding sequence of the bacterial *UidA* gene, which encodes the GUS protein (Jefferson et al., 1987). Transgenic plants containing the *ADF3*pro:*UidA* construct were generated in the accession Col-0 background. Histochemical analysis of GUS activity was performed using X-gluc (5-bromo-4-chloro-3-indolyl-β-D-gluco-pyranosiduronic acid) as the substrate.

Callose Staining

Callose staining and quantification of callose deposits was conducted using a modification of a previously described protocol (Ton and Mauch-Mani, 2004). In brief, leaf samples were cleared overnight in 96% ethanol, followed by a 30-min incubation in sodium phosphate buffer (0.07 M, pH 9). Leaves were then incubated for 60 min in a solution containing 0.005% aniline blue in sodium phosphate buffer (0.07 M, pH 9), followed by the addition of calcofluor to a final concentration of 0.005%. The tissues were immediately observed under a Nikon e600 epifluorescence microscope equipped with a X-cite 120 Fluor System, UV (DAPI) filter and a digital SPOT color camera. Digital images were used to quantify callose spots, which were expressed as number of callose spots per mm^2 of leaf tissue.

Actin Depolymerization Assays

Rabbit skeletal muscle G-actin was prepared by the method of Spudich and Watt (1971) and flash frozen in liquid nitrogen in 0.5 mL aliquots for storage at −70°C until use. After rapid thawing, the G-actin was chromatographed on a superdex 75 gel filtration column immediately prior to measurements. Concentrations of G-actin were determined using an extinction coefficient of 0.63 mg/mL/cm at 290 nm. A portion of the actin was labeled with pyrene iodoacetamide by the method of Cooper et al. (1983) and stored by the same method as the unlabeled G-actin.

Measurements of pyrene-labeled actin were performed with an Aminco-Bowman II luminescence spectrometer using methods similar to those previously described (Xu and Root 2000). In brief, 15% pyrene-labeled actin was polymerized by the addition of 0.1 M KCl and 2 mM $MgCl_2$ yielding a 20-fold enhancement of pyrene fluorescence intensity. Actin concentrations were tested in the ranges of 3 to 7.1 μM for separate experiments. The polymerized actin was titrated at 25°C with a range of concentrations of recombinant GST-tagged ADF3 and ADF4 or buffer as a control, and changes in fluorescence intensity measured. Control experiments indicated a reproducibility of ±10% error or better.

Statistical Analysis

When comparing two treatments or genotypes, two-tail *t* test was used to determine if the mean values were significantly different from each other ($P < 0.05$). When simultaneously comparing multiple genotypes and/or treatments to each other, ANOVA performed following the General Linear model GLM was used followed by Tukey's multiple comparison test to identify mean values that were significantly different from each other ($P < 0.05$; Minitab v15; www.minitab.com). When comparing multiple experimental groups to a single control group, Dunnett's multiple comparison test was used to compare means to identify values that were significantly different ($P < 0.05$) from the control

group. All data conform to the assumptions of ANOVA, and no transformations were necessary. For the EPG analysis, the nonparametric Kruskal-Wallis test (Minitab v15; www.minitab.com) was used to analyze the mean time spent by aphids on various activities.

Accession Numbers

ADF1 (At3g46010); *ADF2* (At3g46000); *ADF3* (At5g59880); *ADF4* (At5g59890); *ADF5* (At2g16700); *ADF9* (At4g34970); *ACT8* (At1g49240); *EF1α* (At5g60390); *PAD4* (At3g52430).

Supplemental Data

The following supplemental materials are available.

Supplemental Figure S1. Arabidopsis lines carrying T-DNA insertions at the *ADF3* locus.

Supplemental Figure S2. *ADF3* expression from the *35S* promoter restores resistance against the GPA in the *adf3-1* mutant.

Supplemental Figure S3. ADF3 exhibits actin-depolymerizing activity.

Supplemental Figure S4. Alignment of ADF3 and ADF4

Supplemental Figure S5. Histochemical staining for GUS activity in uninfested (−GPA) and GPA-infested (+GPA) leaves of a *ADF3*pro:*UidA* plant.

Supplemental Figure S6. Expression of *PAD4* from the constitutively expressed *35S* promoter restores resistance against GPA in plants lacking *ADF3* function.

Supplemental Table S1. Primers used for monitoring gene expression.

ACKNOWLEDGMENTS

The authors thank the Arabidopsis Biological Resource Center for Arabidopsis seeds, Brad Day for *adf1*, *adf3-1*, *adf4*, *adf5*, and *adf9* mutant lines and the *GST-ADF3*, *GST-ADF4*, and *35S:ADF4* clones, Janice de Almeida Engler for the *ADF2*-RNAi line, Zhixiang Chen for the *35S*pro:*PAD4* construct, and Jane Parker and Bart Feys for discussion and making available unpublished results.

Received July 10, 2017; accepted November 9, 2017; published November 10, 2017.

LITERATURE CITED

Andrianantoandro E, Pollard TD (2006) Mechanism of actin filament turnover by severing and nucleation at different concentrations of ADF/cofilin. Mol Cell **24:** 13–23

Blackman RL, Eastop VF (2000) Aphids on the World's Crops: An Identification and Information Guide, Ed 2. John Wiley, Chichester, UK

Bos JIB, Prince D, Pitino M, Maffei ME, Win J, Hogenhout SA (2010) A functional genomics approach identifies candidate effectors from the aphid species *Myzus persicae* (green peach aphid). PLoS Genet **6:** e1001216

Burgos-Rivera B, Ruzicka DR, Deal RB, McKinney EC, King-Reid L, Meagher RB (2008) *ACTIN DEPOLYMERIZING FACTOR9* controls development and gene expression in Arabidopsis. Plant Mol Biol **68:** 619–632

Cai G, Faleri C, Del Casino C, Emons AMC, Cresti M (2011) Distribution of callose synthase, cellulose synthase, and sucrose synthase in tobacco pollen tube is controlled in dissimilar ways by actin filaments and microtubules. Plant Physiol **155:** 1169–1190

Chaturvedi R, Krothapalli K, Makandar R, Nandi A, Sparks AA, Roth MR, Welti R, Shah J (2008) Plastid ω3-fatty acid desaturase-dependent accumulation of a systemic acquired resistance inducing activity in petiole exudates of *Arabidopsis thaliana* is independent of jasmonic acid. Plant J **54:** 106–117

Clément M, Ketelaar T, Rodiuc N, Banora MY, Smertenko A, Engler G, Abad P, Hussey PJ, de Almeida Engler J (2009) Actin-depolymerizing factor2-mediated actin dynamics are essential for root-knot nematode infection of Arabidopsis. Plant Cell **21:** 2963–2979

Cooper JA, Walker SB, Pollard TD (1983) Pyrene actin: Documentation of the validity of a sensitive assay for actin polymerization. J Muscle Res Cell Motil **4:** 253–262

Curtis MD, Grossniklaus U (2003) A gateway cloning vector set for high-throughput functional analysis of genes in planta. Plant Physiol **133:** 462–469

Day B, Henty JL, Porter KJ, Staiger CJ (2011) The pathogen-actin connection: A platform for defense signaling in plants. Annu Rev Phytopathol **49:** 483–506

De Vos M, Jander G (2009) *Myzus persicae* (green peach aphid) salivary components induce defence responses in *Arabidopsis thaliana*. Plant Cell Environ **32:** 1548–1560

Elzinga DA, De Vos M, Jander G (2014) Suppression of plant defenses by a *Myzus persicae* (green peach aphid) salivary effector protein. Mol Plant Microbe Interact **27:** 747–756

Farrants A-KÖ (2008) Chromatin remodelling and actin organisation. FEBS Lett **582:** 2041–2050

Feng Y, Liu Q, Xue Q (2006) Comparative study of rice and Arabidopsis actin-depolymerizing factors gene families. J Plant Physiol **163:** 69–79

Fröhlich A, Gaupels F, Sarioglu H, Holzmeister C, Spannagl M, Durner J, Lindermayr C (2012) Looking deep inside: Detection of low-abundance proteins in leaf extracts of Arabidopsis and phloem exudates of pumpkin. Plant Physiol **159:** 902–914

Garzo E, Soria C, Gomez-Guillamon ML, Fereres A (2002) Feeding behavior of *Aphis gossypii* on resistant accessions of different melon genotypes (*Cucumis melo*). Phytoparasitica **30:** 129–140

Goggin FL (2007) Plant-aphid interactions: Molecular and ecological perspectives. Curr Opin Plant Biol **10:** 399–408

Gottwald JR, Krysan PJ, Young JC, Evert RF, Sussman MR (2000) Genetic evidence for the in planta role of phloem-specific plasma membrane sucrose transporters. Proc Natl Acad Sci USA **97:** 13979–13984

Guerrieri E, Digilio MC (2008) Aphid-plant interactions: A review. J Plant Interact **3:** 223–232

Hafke JB, Ehlers K, Föller J, Höll S-R, Becker S, van Bel AJE (2013) Involvement of the sieve element cytoskeleton in electrical responses to cold shocks. Plant Physiol **162:** 707–719

Hao P, Liu C, Wang Y, Chen R, Tang M, Du B, Zhu L, He G (2008) Herbivore-induced callose deposition on the sieve plates of rice: an important mechanism for host resistance. Plant Physiol **146:** 1810–1820

Henty JL, Bledsoe SW, Khurana P, Meagher RB, Day B, Blanchoin L, Staiger CJ (2011) Arabidopsis actin depolymerizing factor4 modulates the stochastic dynamic behavior of actin filaments in the cortical array of epidermal cells. Plant Cell **23:** 3711–3726

Henty-Ridilla JL, Li J, Blanchoin L, Staiger CJ (2013) Actin dynamics in the cortical array of plant cells. Curr Opin Plant Biol **16:** 678–687

Henty-Ridilla JL, Li J, Day B, Staiger CJ (2014) ACTIN DEPOLYMERIZING FACTOR4 regulates actin dynamics during innate immune signaling in Arabidopsis. Plant Cell **26:** 340–352

Hussey PJ, Ketelaar T, Deeks MJ (2006) Control of the actin cytoskeleton in plant cell growth. Annu Rev Plant Biol **57:** 109–125

Inada N, Higaki T, Hasezawa S (2016) Nuclear function of subclass I Actin-depolymerizing factor contributes to susceptibility in Arabidopsis to an adapted powdery mildew fungus. Plant Physiol **170:** 1420–1434

Jiang C-J, Weeds AG, Hussey PJ (1997) The maize actin-depolymerizing factor, ZmADF3, redistributes to the growing tip of elongating root hairs and can be induced to translocate into the nucleus with actin. Plant J **12:** 1035–1043

Jefferson RA, Kavanagh TA, Bevan MW (1987) GUS fusions: beta-glucuronidase as a sensitive and versatile gene fusion marker in higher plants. EMBO J **6:** 3901–3907

Jockusch BM, Schoenenberger CA, Stetefeld J, Aebi U (2006) Tracking down the different forms of nuclear actin. Trends Cell Biol **16:** 391–396

Kempema LA, Cui X, Holzer FM, Walling LL (2007) Arabidopsis transcriptome changes in response to phloem-feeding silverleaf whitefly nymphs. Similarities and distinctions in responses to aphids. Plant Physiol **143:** 849–865

Kennedy JS, Day MF, Eastop VF (1962) A Conspectus of Aphids as Vectors of Plant Viruses. Commonwealth Institute of Entomology, London

Kulikova AL, Puryaseva AP (2002) Actin in pumpkin phloem exudate. Russ J Plant Physiol **49:** 54–60

Lin M-K, Lee YJ, Lough TJ, Phinney BS, Lucas WJ (2009) Analysis of the pumpkin phloem proteome provides insights into angiosperm sieve tube function. Mol Cell Proteomics **8:** 343–356

Louis J, Leung Q, Pegadaraju V, Reese J, Shah J (2010a) *PAD4*-dependent antibiosis contributes to the *ssi2*-conferred hyper-resistance to the green peach aphid. Mol Plant Microbe Interact **23:** 618–627

Louis J, Lorenc-Kukula K, Singh V, Reese J, Jander G, Shah J (2010b) Antibiosis against the green peach aphid requires the *Arabidopsis thaliana MYZUS PERSICAE-INDUCED LIPASE1* gene. Plant J **64:** 800–811

Louis J, Shah J (2013) *Arabidopsis thaliana-Myzus persicae* interaction: Shaping the understanding of plant defense against phloem-feeding aphids. Front Plant Sci **4:** 213

Louis J, Singh V, Shah J (2012) *Arabidopsis thaliana*-aphid interaction. Arabidopsis Book **10:** e0159

Matthews REF (1991) Relationships between plant viruses and invertebrates. *In* REF Matthews, ed, Plant Virology, Ed 3. Academic Press, New York, pp 520–561

Mittler TE, Dadd RH (1965) Differences in the probing responses of *Myzus persicae* (Sulzer) elicited by different feeding solutions behind a Parafilm membrane. Entomol Exp Appl **8:** 107–122

Miles PW (1999) Aphid saliva. Biol Rev Camb Philos Soc **74:** 41–85

Nalam V, Keeretaweep J, Sarowar S, Shah J (2012) Root-derived oxylipins promote green peach aphid performance on Arabidopsis foliage. Plant Cell **24:** 1643–1653

Nan Q, Qian D, Niu Y, He Y, Tong S, Niu Z, Ma J, Yang Y, An L, Wan D, Xiang Y (2017) Plant actin-depolymerizing factors possess opposing biochemical properties arising from key amino acid changes throughout evolution. Plant Cell **29:** 395–408

Nebl G, Meuer SC, Samstag Y (1996) Dephosphorylation of serine 3 regulates nuclear translocation of cofilin. J Biol Chem **271:** 26276–26280

Nicholson SJ, Hartson SD, Puterka GJ (2012) Proteomic analysis of secreted saliva from Russian wheat aphid (*Diuraphis noxia* Kurd.) biotypes that differ in virulence to wheat. J Proteomics **75:** 2252–2268

Pavlov D, Muhlrad A, Cooper J, Wear M, Reisler E (2007) Actin filament severing by cofilin. J Mol Biol **365:** 1350–1358

Pedigo LP (1999) Entomology and Pest Management, Ed 3. Prentice-Hall, Englewood Cliffs, NJ

Pegadaraju V, Knepper C, Reese JC, Shah J (2005) Premature leaf senescence modulated by the Arabidopsis PHYTOALEXIN DEFICIENT4 gene is associated with defense against the phloem-feeding green peach aphid. Plant Physiol **139:** 1927–1934

Pegadaraju V, Louis J, Singh V, Reese JC, Bautor J, Feys BJ, Cook G, Parker JE, Shah J (2007) Phloem-based resistance to green peach aphid is controlled by *Arabidopsis PHYTOALEXIN DEFICIENT4* without its signaling partner *ENHANCED DISEASE SUSCEPTIBILITY1*. Plant J **52:** 332–341

Pollard DG (1973) Plant penetration by feeding aphids (Hemiptera, Aphidoidea): A review. Bull Entomol Res **62:** 631–714

Pollard TD, Cooper JA (2009) Actin, a central player in cell shape and movement. Science **326:** 1208–1212

Porter K, Shimono M, Tian, M, Day B (2012) Arabidopsis actin-depolymerizing factor-4 links pathogen perception, defense activation and transcription to cytoskeletal dynamics. PLoS Pathog **8:** e1003006

Powell G, Tosh CR, Hardie J (2006) Host plant selection by aphids: Behavioral, evolutionary, and applied perspectives. Annu Rev Entomol **51:** 309–330

Prince DC, Drurey C, Zipfel C, Hogenhout SA (2014) The leucine-rich repeat receptor-like kinase BRASSINOSTEROID INSENSITIVE1-ASSOCIATED KINASE1 and the cytochrome P450 PHYTOALEXIN DEFICIENT3 contribute to innate immunity to aphids in Arabidopsis. Plant Physiol **164:** 2207–2219

Rashid MH, Khan A, Hossain MT, Chung YR (2017) Induction of systemic resistance against aphids by endophytic *Bacillus velezensis*YC7010 via expressing *PHYTOALEXIN DEFICIENT4* in *Arabidopsis*. Front Plant Sci **8:** 211

Rodriguez-Medina C, Atkins CA, Mann AJ, Jordan ME, Smith PMC (2011) Macromolecular composition of phloem exudate from white lupin (*Lupinus albus* L.). BMC Plant Biol **11:** 36

Ruzicka DR, Kandasamy MK, McKinney EC, Burgos-Rivera B, Meagher RB (2007) The ancient subclasses of Arabidopsis Actin Depolymerizing Factor genes exhibit novel and differential expression. Plant J **52:** 460–472

Schobert C, Baker L, Szederkényi J, Grobmann P, Komor E, Hayashi H, Chino M, Lucas WJ (1998) Identification of immunologically related proteins in sieve-tube exudate collected from monocotyledonous and dicotyledonous plants. Planta **206:** 245–252

Schobert C, Gottschalk M, Kovar DR, Staiger CJ, Yoo B-C, Lucas WJ (2000) Characterization of *Ricinus communis* phloem profilin, RcPRO1. Plant Mol Biol **42:** 719–730

Smith CM (2005). Plant Resistance to Arthropods: Molecular and Conventional Approaches. Springer, the Netherlands.

Spudich JA, Watt S (1971) The regulation of rabbit skeletal muscle contraction. I. Biochemical studies of the interaction of the tropomyosin-troponin complex with actin and the proteolytic fragments of myosin. J Biol Chem **246:** 4866–4871

Staiger CJ, Blanchoin L (2006) Actin dynamics: old friends with new stories. Curr Opin Plant Biol **9:** 554–562

Staiger CJ (2000) Signaling to the actin cytoskeleton in plants. Annu Rev Plant Physiol Plant Mol Biol **51:** 257–288

Szymanski DB, Cosgrove DJ (2009) Dynamic coordination of cytoskeletal and cell wall systems during plant cell morphogenesis. Curr Biol **19:** R800–R811

Tian M, Chaudhry F, Ruzicka DR, Meagher RB, Staiger CJ, Day B (2009) Arabidopsis actin-depolymerizing factor AtADF4 mediates defense signal transduction triggered by the *Pseudomonas syringae* effector AvrPphB. Plant Physiol **150:** 815–824

Tjallingii WF (2006) Salivary secretions by aphids interacting with proteins of phloem wound responses. J Exp Bot **57:** 739–745

Ton J, Mauch-Mani B (2004) β-amino-butyric acid-induced resistance against necrotrophic pathogens is based on ABA-dependent priming for callose. Plant J **38:** 119–130

van Helden M, Tjallingii WF (2000) Experimental design and analysis in EPG experiments with emphasis on plant resistance research. *In* GP Walker, EA Backus, eds, Principles and Applications of Electronic Monitoring and Other Techniques in the Study of Homopteran Feeding Behavior. Entomological Society of America, Lanham, MD, pp 144–171.

Vidali L, van Gisbergen PA, Guérin C, Franco P, Li M, Burkart GM, Augustine RC, Blanchoin L, Bezanilla M (2009) Rapid formin-mediated actin-filament elongation is essential for polarized plant cell growth. Proc Natl Acad Sci USA **106:** 13341–13346

Walker GP (2000) A beginner's guide to electronic monitoring of homopteran probing behavior. *In* GP Walker, EA Backus, eds, Principles and Applications of Electronic Monitoring and Other Techniques in the Study of Homopteran Feeding Behavior. Entomological Society of America, Lanham, MD, pp 14–40.

Walling LL (2008) Avoiding effective defenses: Strategies employed by phloem-feeding insects. Plant Physiol **146:** 859–866

Wang W, Wen Y, Berkey R, Xiao S (2009) Specific targeting of the *Arabidopsis* resistance protein RPW8.2 to the interfacial membrane encasing the fungal Haustorium renders broad-spectrum resistance to powdery mildew. Plant Cell **21:** 2898–2913

Will T, Kornemann SR, Furch ACU, Tjallingii WF, van Bel AJE (2009) Aphid watery saliva counteracts sieve-tube occlusion: a universal phenomenon? J Exp Biol **212:** 3305–3312

Will T, Tjallingii WF, Thönnessen A, van Bel AJE (2007) Molecular sabotage of plant defense by aphid saliva. Proc Natl Acad Sci USA **104:** 10536–10541

Will T, van Bel AJE (2006) Physical and chemical interactions between aphids and plants. J Exp Bot **57:** 729–737

Wu Y, Yan J, Zhang R, Qu X, Ren S, Chen N, Huang S (2010) Arabidopsis FIMBRIN5, an actin bundling factor, is required for pollen germination and pollen tube growth. Plant Cell **22:** 3745–3763

Xing X, Chen Z (2006) Effects of mutations and constitutive overexpression of *EDS1* and *PAD4* on plant resistance to different types of microbial pathogens. Plant Sci **171:** 251–262

Xu J, Root DD (2000) Conformational selection during weak binding at the actin and myosin interface. Biophys J **79:** 1498–1510

Ye J, Zheng Y, Yan A, Chen N, Wang Z, Huang S, Yang Z (2009) Arabidopsis formin3 directs the formation of actin cables and polarized growth in pollen tubes. Plant Cell **21:** 3868–3884

Yun BW, Atkinson HA, Gaborit C, Greenland A, Read ND, Pallas JA, Loake GJ (2003) Loss of actin cytoskeletal function and EDS1 activity, in combination, severely compromises non-host resistance in Arabidopsis against wheat powdery mildew. Plant J **34:** 768–777

Zhang X, Henriques R, Lin SS, Niu QW, Chua NH (2006) Agrobacterium-mediated transformation of *Arabidopsis thaliana* using the floral dip method. Nat Protoc **1:** 641–646